

Effects of Anisotropy in QED₃ from Dyson-Schwinger equations in a box

Jacqueline A. Bonnet,¹ Christian S. Fischer,^{1,2} and Richard Williams³

¹*Institut für Theoretische Physik, Universität Giessen, 35392 Giessen, Germany*

²*Gesellschaft für Schwerionenforschung mbH, Planckstr. 1 D-64291 Darmstadt, Germany.*

³*Institut für Physik, Karl-Franzens Universität Graz, Universitätsplatz 5, A-8010 Graz, Austria.*

We investigate the effect of anisotropies in the fermion velocities of 2+1 dimensional QED on the critical number N_f^c of fermions for dynamical mass generation. Our framework are the Dyson-Schwinger equations for the gauge boson and fermion propagators formulated in a finite volume. In contrast to previous Dyson-Schwinger studies we do not rely on an expansion in small anisotropies but keep the full velocity dependence of fermion equations intact. As result we find sizable variations of N_f^c away from the isotropic point in agreement with other approaches. We discuss the relevance of our findings for models of high- T_c superconductors.

I. INTRODUCTION

Quantum electrodynamics in two space and one time dimensions (QED₃) has been studied intensely in the past. QED₃ is a comparably simple quantum field theory which nevertheless displays a rich structure of nonperturbative phenomena such as (a variant of) confinement and dynamical chiral symmetry breaking plus the associated generation of a fermion mass. In condensed matter physics, QED₃ and variants thereof have been suggested as effective theories to describe strongly interacting systems such as high temperature superconductors^{1,2} or graphene^{3,4}.

In the context of high-temperature superconductivity the chirally broken and symmetric phases of QED₃ are associated with the antiferromagnetic spin-density wave state (SDW) and the pseudogap phase of the cuprate compound described as ‘algebraic Fermi liquid’^{1,2}. Here, the fermions of QED₃ represent chargeless quasi-particles, which are low-energy excitations close to the nodes of the (d-wave symmetric) gap-function. These spinons interact with collective, topological excitations of the gap that can be described by a $U(1)$ gauge theory. Furthermore, since the motion of the quasi-particles is confined to the two-dimensional copper-oxide planes in these systems one ends up with quantum electrodynamics in (2+1) dimensions.

There is a long history of debate on the critical number N_f^c of fermions, where the isotropic version of QED₃ undergoes the transition from the chirally broken into the chirally symmetric phase. At zero temperature, if $N_f^c > 2$ then underdoping drives the superconductor directly into the SDW phase, while if $N_f^c < 2$ the system will first go through the pseudogap phase. Indeed, in the continuum studies mostly using Dyson-Schwinger equations^{1,5–8} this number has been found in the range of $N_f^c = 3.5 - 4$ using Ward-identity improved fermion-photon vertices⁸. This range seems to include the critical number extracted from lattice gauge theory^{9–11}, provided the (large) corrections due to the finite lattice volume have been taken into account^{12,13}.

When comparing with the experimental situation, however, isotropic QED₃ may not be the appropriate choice. In fact there are sizable anisotropies in the cuprate compounds due to large differences in the Fermi velocity v_F and a second velocity v_D related to the amplitude of the superconducting order parameter. This fermionic anisotropy can be as

large as¹⁴ $\lambda = v_F/v_D \sim 10$. Furthermore, both velocities are also different from the speed of light, c_s , which is the third scale in the theory. Thus in the effective theory all three Euclidean axes have to be distinguished and it is an important question how and whether the critical number of fermion flavors N_f^c depends on (c_s, v_F, v_D) . In the literature, this situation has begun to be explored in a number of approaches. First studies using renormalisation group and Dyson-Schwinger equations^{1,15} used an expansion only valid for small anisotropies. There it has been concluded that anisotropy is an irrelevant phenomenon in the renormalisation group sense and does not lead to drastic changes in N_f^c . In contrast, lattice gauge theory^{16,17} and a recent study of the strength of the fermion-photon coupling¹⁸ provided evidence for the opposite picture: according to these works anisotropy is relevant and its increase leads to a decrease of the critical number of fermion flavors N_f^c . This opens up the possibility that N_f^c may go down from $N_f^c = 3.5 - 4$ in the isotropic case to $N_f^c < 2$ for values of anisotropy relevant for the high- T_c superconducting systems. However, further studies are necessary to pin down quantitative predictions for this effect.

In this work we reexamine the situation of anisotropic QED₃ from the perspective of Dyson-Schwinger equations. We go beyond the small anisotropy expansions used in Refs.^{1,15} and solve the Dyson-Schwinger equations for the nonperturbative, anisotropic fermion propagator numerically using on the one hand the $1/N_f$ -approximation and on the other hand an improved approximation of the photon propagator as input. These technical details are summarized in section II. Our results, presented in section III, confirm the findings from the lattice^{16,17} and from the fermion-photon coupling strength¹⁸. We discuss qualitative aspects of the dependence of N_f^c on the anisotropies and identify meaningful approximation schemes for the DSEs. We conclude with a summary in section IV.

II. TECHNICAL DETAILS

A. The Dyson-Schwinger equations in anisotropic QED₃

The details of the formulation of anisotropic QED₃ have been discussed in Refs. 1,15,16. Here we only summarize the most important elements using the notation of Ref. 1. The

fermions are represented in the four component spinor representation obeying the Clifford algebra $\{\gamma_\mu, \gamma_\nu\} = 2\delta_{\mu\nu}$. We consider N_f fermion flavors and the anisotropic fermionic velocities v_F and v_Δ which will be included in the metric-like factor $g_{i,\mu\nu}$. In the high-temperature superconducting (HTS) system, the d-wave symmetry of the gap function on the Fermi surface leads to four nodes, which can be grouped into two distinct pairs². This is accounted for by the index $i = 1, 2$. The “metric” is given by:

$$(g_1^{\mu\nu}) = \begin{pmatrix} 1 & 0 & 0 \\ 0 & v_F^2 & 0 \\ 0 & 0 & v_\Delta^2 \end{pmatrix} \quad (1)$$

and

$$(g_2^{\mu\nu}) = \begin{pmatrix} 1 & 0 & 0 \\ 0 & v_\Delta^2 & 0 \\ 0 & 0 & v_F^2 \end{pmatrix}. \quad (2)$$

It enters the Lagrangian in the form of:

$$\mathcal{L}^{aniso} = \frac{N_f}{2} \sum_{j=1,2} \bar{\Psi}_j \left\{ \sum_{\mu=0}^2 \gamma_\mu \sqrt{g_{j,\nu\mu}} (\partial_\mu + i a_\mu) \right\} \Psi_j. \quad (3)$$

As in isotropic QED₃, we can define chiral symmetry using γ_3 and γ_5 . With massless fermions, the Lagrangian therefore has a $U(2N_f)$ “chiral” symmetry, which is broken to $SU(N_f) \times SU(N_f) \times U(1) \times U(1)$ if the fermions become massive. The order parameter for this symmetry breaking is the chiral condensate which can be determined via the trace of the fermion propagator $S_{F,j}(\vec{p}) = \int \frac{d^3x}{(2\pi)^3} e^{i\vec{p}\vec{x}} \langle \bar{\Psi}_j(\vec{x}) \Psi_j(0) \rangle$. The corresponding expression for the photon propagator is given by $D_{\mu\nu}(\vec{p}) = \int \frac{d^3x}{(2\pi)^3} e^{i\vec{p}\vec{x}} \langle A_\mu(\vec{x}) A_\nu(0) \rangle$. The Dyson–Schwinger equations for the fermion and photon propagators are diagrammatically represented as shown in Fig. 1(a) and Fig. 1(b). In Euclidean space-time, they are explicitly given by

$$S_{F,i}^{-1}(\vec{p}) = S_0^{-1}(\vec{p}) + Z_1 e^2 \sum_{i=1,2} \int \frac{d^3q}{(2\pi)^3} (\sqrt{g_{i,\mu\alpha}} \gamma^\alpha S_{F,i}(\vec{q}) \sqrt{g_{i,\nu\beta}} \Gamma^\beta(\vec{q}, \vec{p}) D_{\mu\nu}(\vec{k})), \quad (4)$$

$$D_{\mu\nu}^{-1}(\vec{p}) = D_{0,\mu\nu}^{-1}(\vec{p}) - Z_1 e^2 \frac{N_f}{2} \sum_{i=1,2} \int \frac{d^3q}{(2\pi)^3} \text{Tr} \left[\sqrt{g_{i,\mu\alpha}} \gamma^\alpha S_{F,i}(\vec{q}) \sqrt{g_{i,\nu\beta}} \Gamma^\beta(\vec{p}, \vec{q}) S_{F,i}(\vec{k}) \right], \quad (5)$$

with the momentum \vec{k} defined by the difference $\vec{p} - \vec{q}$ and $i = 1, 2$. Here, the renormalization constant Z_1 of the fermion-boson vertex, $\Gamma^\beta(\vec{p}, \vec{q})$, is included.

As we consider an anisotropic space-time for fermions, we have to take care of dressing each Dirac component separately and also include the node index. In order to keep track more

easily of the general structure of the equations, we introduce some shorthands denoted by

$$\vec{p}_i^2 := p_\mu g_i^{\mu\nu} p_\nu \quad (6)$$

and

$$\tilde{p}_{\mu,i} := A_{\mu,i}(\vec{p}) p_\mu, \text{ (no summation convention!)}, \quad (7)$$

Where $A_{\mu,i}$ denotes the vectorial fermionic dressing function at node i .

The anisotropic expressions for the dressed fermion and photon propagators then read

$$S_{F,i}^{-1}(\vec{p}) = B_i(\vec{p}) + i \sqrt{g_i^{\mu\nu}} \gamma_\nu \tilde{p}_{\mu,i}, \quad (8)$$

$$D_{\mu\nu}(\vec{p})^{-1} = p^2 \left(\delta_{\mu\nu} - \frac{p_\mu p_\nu}{p^2} \right) + \Pi_{\mu\nu}(\vec{p}), \quad (9)$$

where B_i denotes the scalar fermion dressing function at node i and $\Pi_{\mu\nu}(\vec{p})$ the vacuum polarization of the gauge boson field. As the free gauge bosons do not involve fermionic velocities, the bare propagator still is the isotropic one.

In order to close the Dyson–Schwinger equations for the propagators we need to specify the fermion photon vertex Γ^β . This vertex satisfies its own Dyson–Schwinger equation involving a fermion four-point function of which very little is

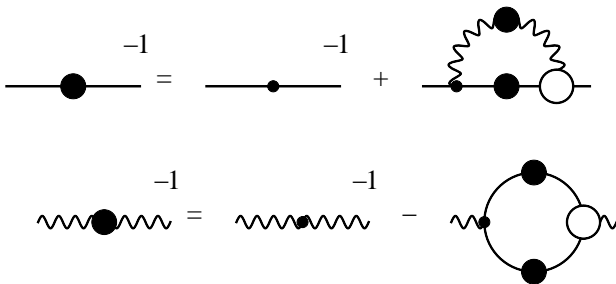


FIG. 1: The diagrammatic representation of the Dyson–Schwinger equations for the fermion (a) and gauge boson propagator (b). Wiggly lines denote photon propagators, straight lines fermion propagators. A blob denotes a dressed propagator or vertex, whereas a dot stands for a bare fermion-photon vertex.

known to date. Strategies to explore the fermion-photon interaction in the isotropic case therefore centered around vertex constructions based on higher order perturbative expansions, multiplicative renormalizability and the Abelian Ward identity^{19–21}. One of the main results of Ref. 8, however, is the stability of the (isotropic) critical number of fermion flavors with respect to the dressing of the vertex: the difference between the values for a bare vertex and much more sophisticated constructions is smaller than five percent. This finding somewhat justifies the use of simple vertex constructions also in the case of anisotropic space-time, where the complexity of the DSEs is large and any simplifications are highly welcome. In this work we therefore employ a vertex construction which only takes into account the leading term of the Ball-Chiu vertex²² (IBC-vertex), generalized to anisotropic space-time. It reads

$$\Gamma_i^\beta(\vec{p}, \vec{q}) = \gamma^\beta \frac{A_i^\beta(\vec{p}) + A_i^\beta(\vec{q})}{2} \quad (10)$$

where no summation convention is used and p, q are the fermion and anti-fermion momenta at the vertex. This vertex is known to be a reasonable approximation to the full Ball-Chiu vertex⁷, which solves the Ward-identity exactly. We will use the vertex Eq. (10) in the quark DSE and also compare results with simpler truncation schemes such as the $1/N_f$ approximation or the Pisarski scheme²³.

In order to make the photon DSE tractable we will use two different approximations: the $1/N_f$ approximation and a more sophisticated model based on the results of Ref. 8. In the limit of isotropic QED₃ there has been extensive work in the $1/N_f$ approximation^{5,6}, which has been found to agree qualitatively with more elaborate approaches⁸. In the anisotropic case the leading order $1/N_f$ approximation has been pursued in Refs. 1,15, where in addition an expansion in terms of small anisotropies has been performed. This is not the case here: we keep the full dependence of the equations on all three velocities (c_s, v_F, v_Δ) . As a result, one may expect to get a rough, but qualitatively correct picture of the effects of anisotropy close to the transition from the chirally symmetric to the chirally broken phase.

The vacuum polarization in leading order large- N_f expansion is given diagrammatically in Fig. 2. The integration can

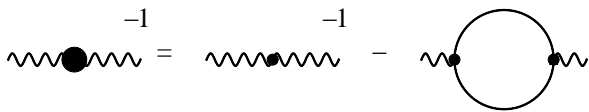


FIG. 2: The diagrammatic representation of the Dyson-Schwinger equation for the vacuum polarization of gauge bosons in leading order large- N_f expansion.

be performed analytically and one obtains^{1,15}:

$$\begin{aligned} \Pi^{\mu\nu}(\vec{p}) &= \sum_i \sqrt{\vec{p}_i^2} \left(g_i^{\mu\nu} - \frac{g_i^{\mu\alpha} p_\alpha g_i^{\nu\delta} p_\delta}{\vec{p}_i^2} \right) \Pi_i(\vec{p}). \\ \Pi_i(\vec{p}) &= \frac{e^2 N_f}{16 v_F v_\Delta} \frac{1}{\sqrt{\vec{p}_i^2}} \end{aligned} \quad (11)$$

Despite its merit of simplicity, there is a serious drawback of the leading order $1/N_f$ -expansion, which makes it desirable to go beyond: it leaves the values of the fermion vector dressing functions $A_i = 1$ at all momenta. In the isotropic case, this behavior is in marked contrast to the one of more sophisticated approximations. There, infrared power laws in A , the photon polarization Π and the quark-photon vertex appear, which are characteristic for the chirally symmetric phase⁸. In addition, in the anisotropic case, non-trivial values of the A -functions at zero momenta serve to define renormalized velocities $(c_s^R, v_F^R, v_\Delta^R)$. It is not clear whether this is possible within the $1/N_f$ -expansion. In order to go beyond this approximation we therefore utilize the results of Ref. 8: in the isotropic case and in the symmetric phase the photon vacuum polarization is well approximated by the following expression:

$$\Pi(k) = \frac{e^2 N_f}{8} \left(\frac{1}{k} \frac{k^2}{k^2 + e^2} + \frac{1}{k^{1+2\kappa}} \frac{e^2}{k^2 + e^2} \right) \quad (12)$$

This expression includes the $1/N_f$ -limit for $\kappa = 0$. In general, however, this anomalous dimension is non-zero and dependent on the details of the vertex truncation. In Ref. 8 the value of κ for the vertex truncation Eq. (10) at the critical number of fermion flavors N_f^c has been determined as $\kappa = 0.0358$. In principle, this number may depend on the fermion velocities in the anisotropic case. Nevertheless, due to our current inability to calculate this dependence we will keep κ constant in all calculations. We therefore arrive at the anisotropic generalization of (12)

$$\Pi_i(\vec{p}) = \frac{e^2 N_f}{16 v_F v_\Delta} \left(\frac{1}{\sqrt{\vec{p}_i^2}} \frac{\vec{p}_i^2}{\vec{p}_i^2 + e^2} + \frac{1}{\vec{p}_i^{1+2\kappa}} \frac{e^2}{\vec{p}_i^2 + e^2} \right) \quad (13)$$

with \vec{p}_i^2 defined in Eq. (6).

In general, we wish to emphasize, that great care has to be taken to use consistent approximations in the photon and fermion DSEs. Either one has to use the $1/N_f$ approximation in both DSEs, leading to the well known isotropic result⁵ $N_f^c \approx 3.24$, or one has to use the vertex Eq. (10) in both DSEs and solve everything self-consistently⁸, leading to $N_f^c \approx 3.56$. Below we will show that we reproduce this last result approximately using our model Eq. (13) for the photon. It is, however, inconsistent and therefore wrong to use the $1/N_f$ -approximation for the photon polarization Eq. (11) and the vertex Eq. (10) in the quark-DSE. This choice leads to $N_f^c \rightarrow \infty$ and therefore prohibits any chiral restoration. We also wish to emphasize that to our mind, meaningful results cannot be extracted from models that violate translation invariance of the photon propagator^{24,25}.

Having specified our approximation (13) of the photon, we now proceed with the fermion-DSE. In order to extract the scalar and vector dressing function of the fermion we take ap-

propriate traces of the fermion-DSE and rearrange the equations to end up with:

$$B_i(\vec{p}) = Z_2 e^2 \int \frac{d^3 q}{(2\pi)^3} \frac{B_i(\vec{q}) g_i^{\mu\nu} D_{\mu\nu}(\vec{k})}{B_i(\vec{q})^2 + (\vec{q}_i)^2} \frac{A_{\mu,i}(\vec{p}) + A_{\mu,i}(\vec{q})}{2}, \quad (14)$$

$$A_{\mu,i}(\vec{p}) = Z_2 - \frac{Z_2 e^2}{p_\mu} \int \frac{d^3 q}{(2\pi)^3} \frac{2 \left(\tilde{q}_{\lambda,i} g_i^{\lambda\nu} D_{\mu\nu}(\vec{k}) \right) - \tilde{q}_{\mu,i} g_i^{\lambda\nu} D_{\lambda\nu}(\vec{k})}{B_i(\vec{q})^2 + (\vec{q}_i)^2} \frac{A_{\mu,i}(\vec{p}) + A_{\mu,i}(\vec{q})}{2}, \quad (15)$$

where again we have no summation for the external index μ . Furthermore we have used the Ward-identity $Z_1 = Z_2$ between the fermion wave function renormalization factor Z_2 and the one for the vertex, Z_1 . The form of the “metric” leads to several symmetries that will simplify the evaluation of the DSEs. In general, we find the relations:

$$B_1(p_0, p_1, p_2) = B_2(p_0, p_2, p_1), \quad (16)$$

$$A_{\mu,1}(p_0, p_1, p_2) = A_{\mu,2}(p_0, p_2, p_1), \quad (17)$$

$$\Pi^{11}(p_0, p_1, p_2) = \Pi^{22}(p_0, p_2, p_1), \quad (18)$$

$$\Pi^{10}(p_0, p_1, p_2) = \Pi^{20}(p_0, p_2, p_1). \quad (19)$$

One then ends end up with eight anisotropic equations that need to be solved self-consistently, in comparison to only three equations for an isotropic space-time. This increase in the number of equations results from the component-wise dressing of the fermion momentum and from the anisotropic vacuum polarization of the gauge bosons. In our case using the $1/N_f$ -approximation or our model (13) in the photon sector we remain with four equations. These reduce to two in the isotropic limit.

B. The DSEs on a torus

Although our approximations of the photon serve to simplify the system of DSEs dramatically, the numerical procedure to solve the remaining equations for $B_1, A_{0,1}, A_{1,1}, A_{2,1}$ is still considerable due to the presence of the anisotropy. In particular, the usual transformation to hyper-spherical coordinates and exploitation of symmetries therein is of course no longer feasible. One possibility to circumvent this problem is to change the base manifold of the system from three-dimensional Euclidean space to that of a three-torus. In Lorenz-covariant systems such a treatment has been explored extensively in the context of QCD^{26,27} and also for QED₃¹³. Here we generalize this treatment to the anisotropic case. In fact, the formulation of DSEs on a torus is ideally suited for this endeavor, since a formulation in Cartesian instead of hyper-spherical coordinates is most natural.

On a compact manifold, the photon and fermion fields have to obey appropriate boundary conditions in the time direction. These have to be periodic for the photon fields and

anti-periodic for the fermions. For computational reasons it is highly advantageous, though not necessary, to choose the same conditions in the spatial directions. We choose the box to be of equal length in all directions, $L_1 = L_2 = L_3 \equiv L$, and denote the corresponding volume $V = L^3$. Together with the boundary conditions this leads to a discretization of momentum space. Thus all momentum integrals appearing in the Dyson-Schwinger equations are replaced by sums over Matsubara modes. For the fermions this amounts to

$$\int \frac{d^3 q}{(2\pi)^3} (\dots) \rightarrow \frac{1}{L^3} \sum_{n_1, n_2, n_3} (\dots), \quad (20)$$

counting momenta $\mathbf{q}_n = \sum_{i=1..3} (2\pi/L)(n_i + 1/2)\hat{e}_i$, where \hat{e}_i are Cartesian unit vectors in Euclidean momentum space. For the photon with periodic boundary conditions the momentum counting goes like $\mathbf{q}_n = \sum_{i=1..3} (2\pi/L)(n_i)\hat{e}_i$. The resulting system of equations can be solved numerically along the lines described in Ref. 13.

Of course, working on a torus with a finite volume introduces artifacts. These have been studied in some detail in Ref. 13, and found to be sizable, see Fig. 7 of this reference. In addition, nonlinear volume effects have been found for very large volumes in Ref. 12. The reason for these large effects is the large separation of scales in QED₃. Besides the natural scale $e^2 = 1$ of the coupling with dimension one, there is the scale of dynamical mass generation which even well in the broken phase is at least two orders of magnitude below the natural scale. This is a situation totally different to, e.g., QCD where both scales are of the same order. In the isotropic theory, the large volume effects in QED₃ explain why lattice simulations^{9–11} find critical numbers of fermion flavors of the order of $N_f^c \approx 1.5$, while continuum calculations in the DSE framework⁸ find $N_f^c \approx 3.5$. The DSE calculations on the torus explained these two results as a consequence of the finite lattice volume¹³. We will briefly address the corresponding volume effects in the anisotropic case in section III C. We find indications, that the size of the volume effects is hardly affected by changes of the fermion velocities, at least in the range relevant for our study. Thus while the absolute number for N_f^c on the torus needs to be corrected, its variation with (c_s, v_F, v_Δ) is nevertheless meaningful. We therefore adopt a similar strategy as the authors of Ref. 18 and concentrate on

the variations rather than the absolute value of N_f^c .

III. NUMERICAL RESULTS

In this section we will discuss our numerical results for three different approximation schemes. For the fermion DSE these are (i) the Pisarski scheme²³, (ii) the leading order $1/N_f$ expansion and (iii) our most elaborate scheme using the vertex Eq. (10) and the photon model Eq. (13). Before we present our results for the isotropic and anisotropic cases at finite volume, we briefly discuss the corresponding infinite volume results in the isotropic case. In general, besides the chiral condensate another suitable order parameter for chiral symmetry breaking is the value of the scalar fermion dressing function at any point in momentum space; here we use $B(\vec{p})$ at the smallest momentum available.

A. The critical N_f^c in the isotropic case

In the Pisarski scheme, analysed in detail in Ref. 23, the fermion-photon vertex is set to the bare one and the scalar dressing function of the fermion is set to a constant, $B(\vec{p}) = B(0) = m$. This rough approximation scheme is well suited to analytically demonstrate that chiral symmetry is broken in QED₃. As a result one obtains

$$m = B(0) = c \alpha e^{-\pi^2 N_f / 8}, \quad (21)$$

where c is a positive constant and $\alpha = e^2 N_f$. Clearly, chiral symmetry is broken and remains broken for any value of N_f . Thus $N_f^c \rightarrow \infty$, which is in contrast to the findings in more elaborate approximation schemes. Therefore, although the Pisarski scheme served as a nice tool for demonstrating broken chiral symmetry in the first place, it is not well suited to extract information on chiral symmetry restoration. We will see below that this remains true in the anisotropic case.

Let us now focus on the other two approximation schemes (ii) and (iii). In the infinite volume limit the dependence of $B(0)$ on N_f has been determined in Ref. 8 together with results for more elaborate vertex truncations. Here we combine the result for our photon model Eq. (13) together with the vertex approximation Eq. (10). In Fig. 3, we display our results. For all three truncations we clearly find an exponential decrease of the order parameter with N_f , a situation described as Miransky-scaling²⁸ in the literature. (Note that universal power law corrections to Miransky scaling have been discussed in Ref. 29 and Refs. therein. For QED₃ the quantitative aspects of these corrections have not yet been studied.) The critical number N_f^c has been determined analytically for the $1/N_f$ and the self-consistent 1BC-vertex truncations: $N_f^{c,1/N_f} \approx 3.24$ and $N_f^{c,1BC} \approx 3.56$. The corresponding value for our model $N_f^{c,model}$ is a little lower than the one for the $1/N_f$ -approximation, as can be inferred from Fig. 3.

The reason why $N_f^{c,model} \neq N_f^{c,1BC}$ is the following: the photon in the self-consistent 1BC-approximation is a constant in the infrared for $N_f < N_f^c$ and develops an infrared

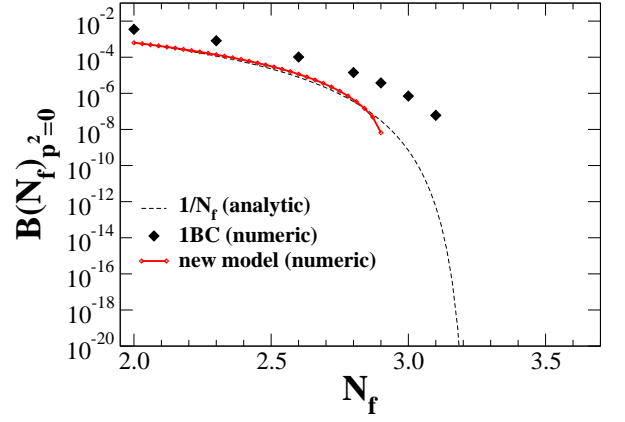


FIG. 3: The order parameter for chiral symmetry breaking, $B(0)$, plotted as a function of the number of fermion flavours N_f in the isotropic case $1 = c_s = v_F = v_\Delta$. Shown are results for the self-consistent leading order $1/N_f$ -approximation and the 1BC-vertex, Eq. (10), compared with the results for our model Eq. (13) for the photon together with the vertex Eq. (10) in the fermion-DSE.

power law for $N_f > N_f^c$. In our model, the power law is already present for $N_f < N_f^c$, which results in missing infrared strength and therefore explains why $N_f^{c,model} < N_f^{c,1BC}$. This is, however, only a small quantitative effect which is irrelevant for the qualitative study presented in this work.

B. The critical N_f^c in the anisotropic case

In this section we discuss the general anisotropic case with $c_s = 1$ and (v_F, v_Δ) varied. We first investigate the Pisarski approximation, which has been used in Ref. 18 to argue for a couple of general points. Again, similar to the isotropic case, we can determine the behavior of the order parameter analytically, at least for $v_F = v_\Delta$. The details are reported in appendix A. We find

$$m = B(0) = c \alpha \exp \left[\left(-\pi^2 N_f \sqrt{v_F^2 - 1} \right) / \left(2\sqrt{v_F^2 - 1} + 2(2 + v_F^2) \arctan(\sqrt{v_F^2 - 1}) \right) \right], \quad (22)$$

which is different to the corresponding expression reported in Ref. 18. Our result has the correct isotropic limit and it generalises the finding from the isotropic case: in the Pisarski approximation (and for $d = 3$ dimensions) chiral symmetry is always broken, i.e. $N_f^c \rightarrow \infty$. We therefore find this approximation not to be suited in general to extract quantitative information on the variation of N_f^c with (c_s, v_F, v_Δ) .

We now proceed with our two more elaborate approximations. In Figs. 4 and 5 we show our results on a torus with $e^2 = 1$, $L = 600/e^2$ and 20^3 momentum points. The values of N_f^c are represented by contour lines and a corresponding color code. Note that the ‘edges’ in the contour lines are due to the sparseness of our grid in some regions; in general we expect smooth lines in the v_F - v_Δ -space. For $v_F = v_\Delta = 1$ we

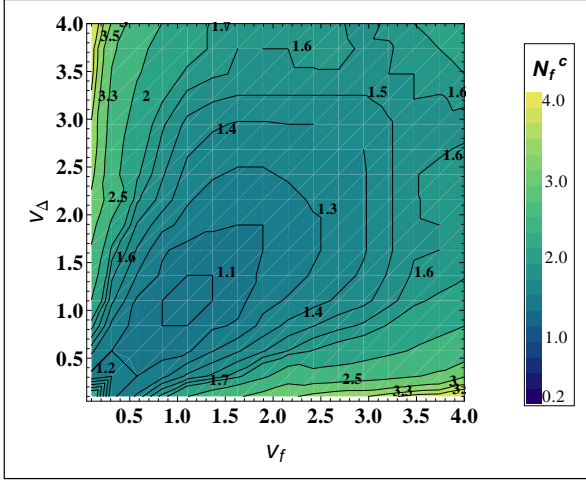


FIG. 4: Critical number of fermion flavours N_f^c determined in the $1/N_f$ -approximation and plotted as a function of the fermion velocities (v_F, v_Δ) .

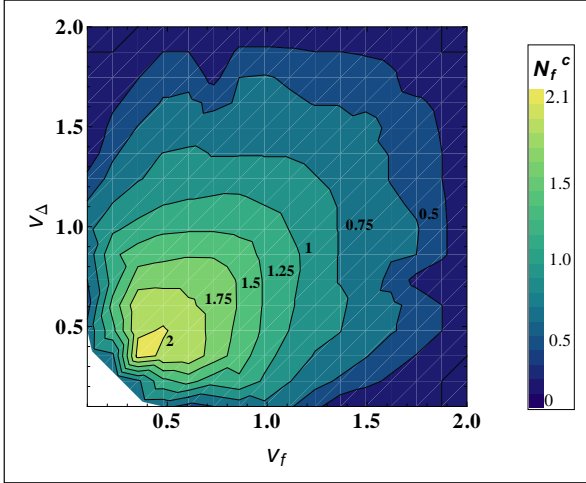


FIG. 5: Critical number of fermion flavours N_f^c determined from the photon model Eq. (13) and the fermion-photon vertex Eq. (10) plotted as a function of the fermion velocities (v_F, v_Δ) .

can read off the corresponding values for N_f^c in the isotropic case. We find $N_f^{c,1/N_f} \approx 1.0$ and $N_f^{c,model} \approx 1.1$. Clearly, these values are affected by large finite volume effects, as already discussed above. When we compare these with the corresponding values in the continuum calculation we find that the latter are roughly a factor of three larger. This has to be kept in mind when discussing Figs. 4 and 5.

For non-trivial values of v_F and v_Δ we find sizable deviations of N_f^c from the isotropic case. We also observe that the two truncation schemes behave very differently. In general the $1/N_f$ -approximation shows an increase of the critical number of fermions with respect to deviations from the isotropic case in all directions. This finding is in agreement with early expectations¹⁵ from Dyson-Schwinger equations, performed

in the $1/N_f$ -expansion and furthermore in an expansion of small anisotropies. Thus what we have shown here is that the results of Ref. 15 survive also for large anisotropies. There remains, however, the question of the reliability of the $1/N_f$ -expansion. We have already discussed above, that the leading order $1/N_f$ -expansion contains the approximation $A_i = 1$, which is certainly not valid in general. Our modified approximation scheme Eq. (10) and Eq. (13) avoids this problem. Indeed, our results for N_f^c in this model show a different behavior. Here we find a maximum of N_f^c for small values of (v_F, v_Δ) at or around $(v_F, v_\Delta) = (0.4, 0.4)$ with decreasing behavior for smaller and larger velocities. In the region where both velocities are smaller than $c_s = 1$ the critical number of fermions never goes to zero. This is different for large velocities: in fact if one of the velocities is larger than a certain critical value of the order of $v_F, v_\Delta \approx 2$, the system is always in the chirally symmetric phase. Certainly the precise number, where this happens, is expected to be severely affected by volume effects. Nevertheless, this qualitative behavior is in good agreement with the corresponding evaluation performed in Ref. 18, where the criterion of the strength of one-photon exchange between fermions was used. Our results therefore corroborate their findings. (It is perhaps amusing to note that in Ref. 18 the statement was made that it is ‘almost impossible’ to analyze mass generation in the presence of anisotropies using Dyson-Schwinger equations. Naturally, in the light of this work we do not agree with this statement.) As argued in detail in Ref. 18, the picture indicated by Fig. 5 is also supported by lattice calculations^{16,17}. In the light of this agreement we tend to the statement that the $1/N_f$ -approximation picture of Fig. 4 is misleading and has to be discarded.

C. Volume effects and the case $v_F/v_\Delta \sim 10$

Let us now briefly come back to the volume effects associated with our calculation on the torus. In Ref. 13 these effects have been analyzed in the isotropic case and tori as large as $N = 512^3$ have been used. In the anisotropic case the numerical effort to determine N_f^c is much larger than in the isotropic case and the $N = 20^3$ calculations reported above are already demanding in terms of CPU time. A detailed and concise study of the volume effects using large tori is therefore beyond the scope of the present work. Nevertheless we wish to demonstrate, that the assumption used above, namely that the size of the volume effects do not too strongly depend on the size of the anisotropy, may be correct. To this end we show the results for four selected points on the $v_F = v_\Delta$ -axis for $N = 30^3$ in Fig. 6. Clearly, the larger volume results in a larger value for N_f^c , as visible from the plot. Comparing the volume effects at the isotropic point with the value at $v_F = 1.5$ we find quantitative differences, but certainly not too different to invalidate our assumption from the last section on a qualitative level. Finally we also observe, that the line of demarcation from $N_f^c \neq 0$ to $N_f^c = 0$ moves strongly with volume. Clearly, further studies are necessary to pin down the size of the volume effects to such an extent, that extrapolations to the infinite volume limit along the lines of Ref. 13 are

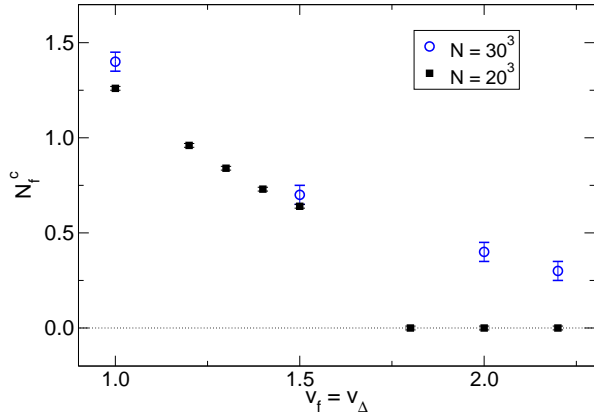


FIG. 6: Four selected points on the $v_F = v_\Delta$ -axis determined with two different tori with $N = 20^3$ and $N = 30^3$ corresponding to box lengths of $Le^2 = 600$ and $Le^2 = 900$.

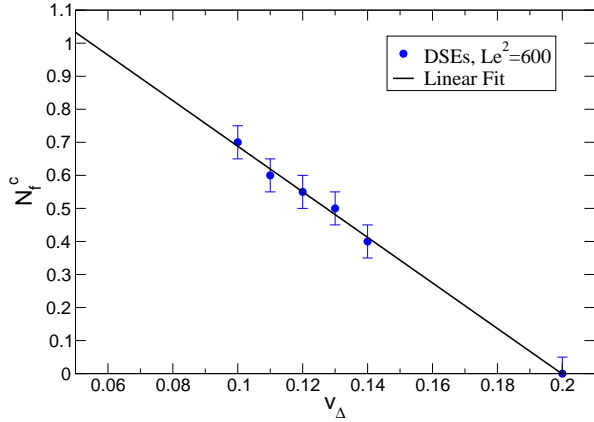


FIG. 7: Selected results for the critical number of fermion flavors at $(v_F, v_\Delta) = (10v_\Delta, v_\Delta)$ from a torus with $Le^2 = 600$. The error bars correspond to our step size when searching for N_f^c .

possible. To forego the problem of finite volume effects, one may also attempt to solve the equations directly in the infinite volume continuum limit. We will report on first results in this direction elsewhere.

When comparing with experiment, values of (v_F, v_Δ) of the order of $\lambda = v_F/v_\Delta \sim 10$ may be of particular interest; Ref. 14 reports $\lambda = 14$ for optimally doped $\text{YBa}_2\text{Cu}_3\text{O}_7$ and $\lambda = 19$ for $\text{Bi}_2\text{Sr}_2\text{CaCu}_2\text{O}_8$ compounds. In addition, it is important to know the relation of (v_F, v_Δ) to the speed c_s related with the gauge boson. Here, we recall that c_s is not the speed of light in the cuprate compound, but the speed characteristic for the vortex-antivortex excitations that are represented by the gauge field in the effective theory. It is thus possible and even anticipated that $v_F > c_s$, as discussed in Ref. 18. To our knowledge, the precise relation of v_F and c_s is not yet determined from experiment. We therefore show results for $(10v_\Delta, v_\Delta)$ in a typical range accessible in our

calculation in Fig. 7. The filled circles in the plots are our numerical results, whereas the black line is a linear fit to the data points. Clearly, the dependence of N_f^c on v_Δ is well approximated by this fit. Whether this linear dependence remains intact in the infinite volume limit should be studied in future work.

IV. SUMMARY AND CONCLUSIONS

In this work we have proposed an approximation for the Dyson-Schwinger equations of QED_3 , which is well suited to investigate the effects of anisotropies on the critical number of fermion flavors for chiral symmetry restoration. This problem is important for the description of high T_c cuprate superconductors using QED_3 as an effective theory. Our results support corresponding ones from lattice calculations^{16,17} and continuum studies of the fermion-photon interaction strength¹⁸. In our best approximation scheme we find a maximum of the critical number of fermion flavors N_f^c around $v_F = v_\Delta \approx 0.5$. From this point, N_f^c is decreasing in all directions in the (v_F, v_Δ) -plane. Further studies, however, are necessary to pin down the quantitative aspects of this behavior. Our results are still preliminary in at least three aspects. They are affected by large volume effects, which have been studied in detail only at the isotropic velocity point¹³. Our calculation is certainly affected by truncation errors in the fermion-photon vertex, although we have argued from comparison with more systematic calculations at the isotropic point⁸, that these effects are on a moderate level of the order of twenty to thirty percent. Finally, our treatment of the anisotropic photon DSE remains preliminary and a more self-consistent calculation is certainly desirable. Nevertheless, we believe that the qualitative aspects of our results are correct and provide a further step forward to understand the connection between QED_3 and experimental studies of high T_c superconductors.

Acknowledgement

This work was supported by the Helmholtz-University Young Investigator Grant No. VH-NG-332 and by the Deutsche Forschungsgemeinschaft through SFB 634.

Appendix A: Anisotropic N_f^c in the Pisarski approximation

In this appendix we give some details to the dependence of the fermion mass on the number of flavors in the Pisarski approximation. For $v_F = v_\Delta$, we insert the large- N_f vacuum polarization, Eq. (11), into the scalar fermion dressing function given implicitly in Eq. (4). For equal fermionic velocities, we make use of the inherent symmetry and switch to cylindrical coordinates. With the abbreviations

$$\begin{aligned}
\mathcal{A} &= 2v_F^6 z^4 (\sqrt{r^2 + z^2} \alpha^2 + 16z^2 (4\sqrt{r^2 + z^2} + \alpha)) + 8r^6 (8\sqrt{r^2 + z^2} + \alpha + v_F^2 (8\sqrt{r^2 + z^2} + 3\alpha)) \\
\mathcal{B} &= r^2 v_F^2 z^2 ((1 + v_F^2)^2 \sqrt{r^2 + z^2} \alpha^2 + 8z^2 (8\sqrt{r^2 + z^2} + 24v_F^2 \sqrt{r^2 + z^2} + 16v_F^4 \sqrt{r^2 + z^2} + (2 + 5(v_F^2 + v_F^4))\alpha)) \\
\mathcal{C} &= 2r^4 (v_F^2 \sqrt{r^2 + z^2} \alpha^2 + 4z^2 (8\sqrt{r^2 + z^2} + \alpha + v_F^2 (16\sqrt{r^2 + z^2} + 24v_F^2 \sqrt{r^2 + z^2} + (5 + 5v_F^2 + v_F^4)\alpha))) \\
\mathcal{D} &= N_f (r^2 + z^2) (r^2 + v_F^2 z^2)^2 (8\sqrt{r^2 + z^2} + \alpha) \\
\mathcal{E} &= 64r^4 + r^2 (64(1 + v_F^2)z^2 + 8\sqrt{r^2 + z^2} \alpha + v_F^2 \alpha (8\sqrt{r^2 + z^2} + \alpha)) + v_F^2 z^2 (64z^2 + \alpha (16\sqrt{r^2 + z^2} + \alpha))
\end{aligned}$$

we arrive at

$$B(\vec{p}) = \frac{1}{(2\pi)^3} \int_0^{2\pi} \int_0^\infty \int_0^\infty d\varphi dr dz \frac{16 B(\vec{p}) r \alpha (\mathcal{A} + \mathcal{B} + \mathcal{C})}{\mathcal{D} \mathcal{E}}. \quad (\text{A1})$$

At this point we perform Pisarski's approximation²³ and set the scalar fermion dressing function $B(\vec{p})$ equal to a constant

$B(\vec{p}) = m$ for all momenta in the range $\alpha \gg p \gg m$. Other momentum contributions are neglected in the integration. Furthermore, since $r < \alpha$ and $q < \alpha$ we only keep terms with the largest power of α in the numerator and denominator of the integrand. This leads to the more compact equation

$$m = \frac{1}{(2\pi)^3} \int_0^{2\pi} d\varphi \int_m^\alpha dr \int_m^\alpha dz \frac{16mr (2r^4 + r^2(1 + v_F^2)z^2 + 2v_F^4 z^4)}{N_f (r^2 + z^2)^{\frac{3}{2}} (r^2 + v_F^2 z^2)^2}. \quad (\text{A2})$$

As a next step, we perform the z integral and again neglect the terms not proportional to α . We end up with

$$m = \frac{1}{(2\pi)^3} \int_0^{2\pi} d\varphi \int_m^\alpha dr \frac{8m (\sqrt{v_F^2 - 1} \alpha + (2 + \alpha) \arctan[\sqrt{v_F^2 - 1}])}{N_f r \alpha \sqrt{v_F^2 - 1}}. \quad (\text{A3})$$

We further perform the r and φ integral and use one last time that α is the largest scale in the problem. We finally arrive at

$$m = \frac{2m (\sqrt{1 + v_F^2} + (2 + v_F^2) \arctan(\sqrt{1 + v_F^2}))}{\pi^2 N_f \sqrt{1 + v_F^2}} \ln \left(\frac{\alpha}{m} \right), \quad (\text{A4})$$

which leads to the result given in the main text, Eq. (22):

$$m = B(0) = c \alpha \exp \left[\left(-\pi^2 N_f \sqrt{v_F^2 - 1} \right) / \left(2\sqrt{v_F^2 - 1} + 2(2 + v_F^2) \arctan(\sqrt{v_F^2 - 1}) \right) \right].$$

¹ M. Franz, Z. Tesanovic and O. Vafek, Phys. Rev. B **66** (2002) 054535 [arXiv:cond-mat/0203333]; Z. Tesanovic, O. Vafek, and M. Franz, Phys. Rev. B **65** (2002) 180511 [arXiv:cond-mat/0110253]; M. Franz and Z. Tesanovic, Phys. Rev. Lett. **87**, (2001) 257003. [arXiv:cond-mat/0012445];

² I. F. Herbut, Phys. Rev. B **66**, 094504 (2002) [arXiv:cond-mat/0202491]; Phys. Rev. Lett. **88** (2002) 047006 [arXiv:cond-mat/0110188].

³ K. S. Novoselov, A. K. Geim, S. V. Morozov, D. Jiang, M. I. Kat-

snelson, I. V. Grigorieva, S. V. Dubonos, A. A. Firsov, Nature **438** (2005) 197. [arXiv:cond-mat/0509330 [cond-mat.mes-hall]].

⁴ V. P. Gusynin, S. G. Sharapov and J. P. Carbotte, Int. J. Mod. Phys. B **21**, 4611 (2007) [arXiv:0706.3016 [cond-mat.mes-hall]].

⁵ T. Appelquist, D. Nash and L. C. R. Wijewardhana, Phys. Rev. Lett. **60** (1988) 2575.

⁶ D. Nash, Phys. Rev. Lett. **62** (1989) 3024.

⁷ P. Maris, Phys. Rev. D **54** (1996) 4049 [arXiv:hep-ph/9606214].

⁸ C. S. Fischer, R. Alkofer, T. Dahm and P. Maris, Phys. Rev. D **70**

- (2004) 073007 [arXiv:hep-ph/0407104].
- ⁹ S. J. Hands, J. B. Kogut and C. G. Strouthos, Nucl. Phys. B **645** (2002) 321 [arXiv:hep-lat/0208030].
 - ¹⁰ S. J. Hands, J. B. Kogut, L. Scorzato and C. G. Strouthos, Phys. Rev. B **70** (2004) 104501 [arXiv:hep-lat/0404013].
 - ¹¹ C. Strouthos and J. B. Kogut, arXiv:0808.2714 [cond-mat.supr-con]; C. Strouthos and J. B. Kogut, PoS **LAT2007** (2007) 278 [arXiv:0804.0300 [hep-lat]].
 - ¹² V. P. Gusynin and M. Reenders, Phys. Rev. D **68** (2003) 025017 [arXiv:hep-ph/0304302].
 - ¹³ T. Goecke, C. S. Fischer and R. Williams, Phys. Rev. B **79** (2009) 064513 [arXiv:0811.1887 [hep-ph]].
 - ¹⁴ M. Chiao, R. W. Hill, C. Lupien, L. Taillefer, P. Lambert, R. Gagnon, P. Fournier, Phys. Rev. B **62** (2000) 3554
 - ¹⁵ D. J. Lee and I. F. Herbut, Phys. Rev. B **66**, 094512 (2002) [arXiv:cond-mat/0201088].
 - ¹⁶ S. Hands and I. O. Thomas, Phys. Rev. B **72**, 054526 (2005) [arXiv:hep-lat/0412009].
 - ¹⁷ I. O. Thomas and S. Hands, Phys. Rev. B **75**, 134516 (2007) [arXiv:hep-lat/0609062]; PoS **LAT2005**, 249 (2006) [arXiv:hep-lat/0509038].
 - ¹⁸ A. Concha, V. Stanev and Z. Tesanovic, Phys. Rev. B **79** (2009) 214525 [arXiv:0906.1103 [cond-mat.supr-con]].
 - ¹⁹ D. C. Curtis, M. R. Pennington, Phys. Rev. **D42** (1990) 4165-4169.
 - ²⁰ A. Bashir, A. Kizilersu, M. R. Pennington, [hep-ph/9907418].
 - ²¹ A. Kizilersu, M. R. Pennington, Phys. Rev. **D79** (2009) 125020. [arXiv:0904.3483 [hep-th]].
 - ²² J. S. Ball, T. -W. Chiu, Phys. Rev. **D22** (1980) 2542.
 - ²³ R. D. Pisarski, Phys. Rev. D **29** (1984) 2423.
 - ²⁴ A. Bashir, A. Raya, I. C. Cloet and C. D. Roberts, Phys. Rev. C **78** (2008) 055201 [arXiv:0806.3305 [hep-ph]].
 - ²⁵ A. Bashir, A. Raya, S. Sanchez-Madrigal, C. D. Roberts, Few Body Syst. **46** (2009) 229-237. [arXiv:0905.1337 [hep-ph]].
 - ²⁶ C. S. Fischer, R. Alkofer and H. Reinhardt, Phys. Rev. D **65** (2002) 094008 [arXiv:hep-ph/0202195]; C. S. Fischer, B. Gruter and R. Alkofer, Annals Phys. **321** (2006) 1918 [arXiv:hep-ph/0506053]; C. S. Fischer, A. Maas, J. M. Pawłowski and L. von Smekal, Annals Phys. **322**, 2916 (2007) [arXiv:hep-ph/0701050].
 - ²⁷ C. S. Fischer and M. R. Pennington, Phys. Rev. D **73** (2006) 034029 [arXiv:hep-ph/0512233]; Eur. Phys. J. A **31** (2007) 746 [arXiv:hep-ph/0701123]; J. Luecker, C. S. Fischer and R. Williams, Phys. Rev. D **81** (2010) 094005 [arXiv:0912.3686 [hep-ph]].
 - ²⁸ V. A. Miransky, K. Yamawaki, Mod. Phys. Lett. **A4** (1989) 129-135; Phys. Rev. **D55** (1997) 5051-5066. [hep-th/9611142].
 - ²⁹ J. Braun, C. S. Fischer, H. Gies, [arXiv:1012.4279 [hep-ph]].